

Received: 17.04.2025

Accepted: 20.05.2025

Research Article

The Development and Theoretical Examination of Hplc-Ms Determination Method For A Novel Veterinary Drug Tryfuzol-Neo 1% In Meat And Animal Organs

Volodymyr Parchenko^a, Alireza Poustforoosh^b, Yuri Karpenko^{a,1}, Boris Kyrychko^c, Burak Tüzün^{d,2}, Elena Kyrychko^c, Tatiana Chetvertak^e, İlayda Bersu Kul^f

^aDepartment of toxicological and inorganic chemistry, Zaporizhzhya state medical university, 69600, Mayakov'sky Ave, 26, Zaporizhzhya, Ukraine

^bMedicinal and Natural Products Chemistry Research Center, Shiraz University of Medical Sciences, Shiraz, Iran

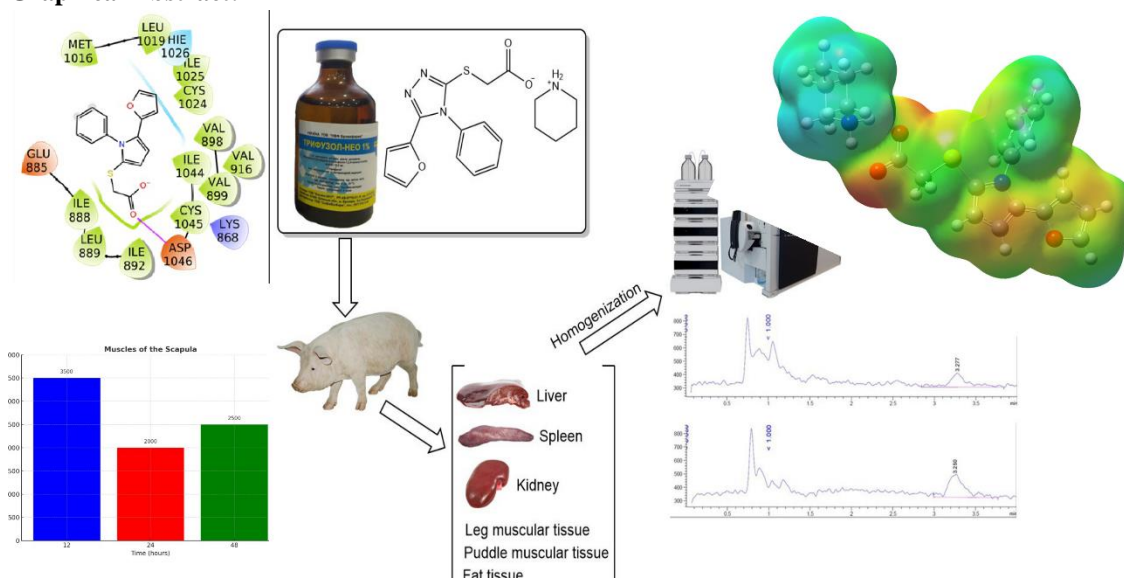
^cDepartment of surgery and obstetrics, Poltava State Agrarian Academy, 36000, Skovorody Str. 1, Poltava Ukraine

^dPlant and Animal Production Department, Technical Sciences Vocational School of Sivas, Sivas Cumhuriyet University, 58140, Sivas, Turkey

^eDepartment of Chemistry and Chemical Education, Bogdan Khmelnytsky Melitopol State Pedagogical University, Melitopol, Ukraine

^fDepartment of Molecular Biology and Genetics, Science Faculty, Sivas Cumhuriyet University, 58140, Sivas, Turkey

Graphical Abstract:



Abstract: This study aimed to develop and validate an HPLC-MS method for determining Tryfuzol-neo 1% (piperidinium- $\{[5-(2\text{-furan-4-phenyl-4H-1,2,4-triazole-3-ylthio})\text{acetate}]\}$) in food control, veterinary, and biological samples, while also investigating its molecular interactions with cancer targets. A novel HPLC-MS methodology was developed and successfully applied to quantify Tryfuzol-neo residues in meat and

¹ Corresponding Authors

e-mail: karpenko.y.v@gmail.com

² Corresponding Authors

e-mail: theburaktuzun@yahoo.com

Volodymyr Parchenko, Alireza Poustforoosh, Yuri Karpenko, Boris Kyrychko, Burak Tüzün, Elena Kyrychko, Tatiana Chetvertak, İlayda Bersu Kul

animal organ matrices. Complementary computational studies were conducted using Gaussian calculations at B3LYP, HF, and M062X levels with 6-31g, 6-31++g, and 6-31++g(d,p) basis sets to examine the compound's properties. Molecular docking and dynamics simulations revealed stable binding interactions between Tryfuzol-neo and six cancer-related proteins: 2JW2, 2H80, and 3WZE (liver cancer); 2XIR and 5C5S (kidney cancer); and 3VF8 (spleen cancer). The results demonstrate the method's effectiveness for detecting Tryfuzol-neo in complex biological samples, while the computational analyses suggest potential therapeutic applications through specific protein interactions. This work presents the first validated HPLC-MS protocol for Tryfuzol-neo detection in food safety and veterinary medicine contexts, with the additional finding of its promising binding affinity to multiple cancer targets. The combination of analytical and in silico approaches provides a comprehensive characterization of Tryfuzol-neo, supporting its potential dual use as both a veterinary drug and a candidate for further anticancer research. These findings warrant additional pharmacological studies to explore Tryfuzol-neo's therapeutic potential and mechanism of action against the investigated cancer types.

Keywords: Tryfuzol-neo, HPLC-MS analytical method, pharmaceutical analysis, veterinary and toxicological analysis, In silico

1. Introduction

The 1,2,4-triazoles represent a wide spectrum of biological activities [1–15]. Nowadays, different novel drugs, containing 1,2,4-triazoles as active substances have been developed and registered [16–28].

Among them, “Trifuzol-neo 1%-neo 1%” (the active substance is piperidinium-([5-(2-furan)-4-phenyl-4H-1,2,4-triazole-3-ylthio)acetate is the new generation drug with hepatoprotecting, cardioprotecting, antioxidant, immunomodulating, interferonogenic,

antiinflammatory, detoxication, pain-relieving action. It is used in treatment of all types of fertile and eunuch cattle and aviculture. It has shown its effectiity against corona-rota, rheo-, paramixo-, picorna-, parvo-, circo-, herpa- and other viral infections [16]. It may be used either in prophylaxis or in complex therapy with other drugs like antibiotics and vitamins. Its active substance is piperidinium-([5-(2-furan)-4-phenyl-4H-1,2,4-triazole-3-ylthio)acetate in Figure 1. Its action is dose-related, thus the development of a method of its quantification in different forms is really actual.

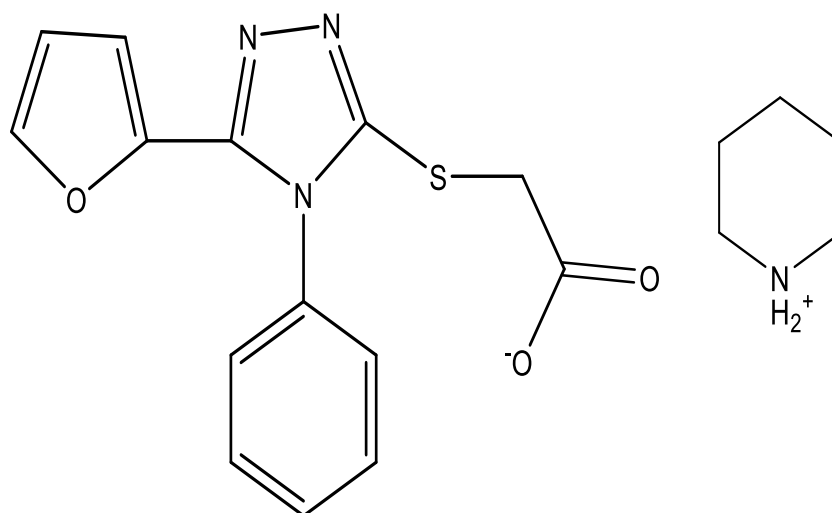


Figure 1. Tryfuzol-neo 1% active ingredient

Gaussian is a powerful software widely used for quantum chemistry and molecular modeling. It is used to calculate energy states, molecular structures, vibrational frequencies, and other

properties of chemical systems [17]. Gaussian offers the possibility of modeling chemical processes with different theoretical approaches such as Hartree-Fock (HF), density functional

Volodymyr Parchenko, Alireza Poustforoosh, Yuri Karpenko, Boris Kyrychko, Burak Tüzün, Elena Kyrychko, Tatiana Chetvertak, İlayda Bersu Kul

theory (DFT), and molecular mechanics (MM). In particular, it is an important tool for understanding reaction mechanisms and energy profiles.

Molecular docking is a computer simulation method that predicts the binding form and energy of a ligand to a target protein or molecular structure [18]. This technique is critical for drug discovery and design. Docking usually involves binding energy calculations and molecular interaction analyses to determine how the ligand binds to the active site of the target [19]. For example, hydrophobic, hydrogen bonding, and electrostatic interactions are the main factors evaluated in docking simulations [20].

Molecular dynamics simulations are a method used to study the physical motions between atoms and molecules over time. MD simulates the dynamics of atoms and molecules based on Newton's equations of motion and allows observing structural and thermodynamic changes over time [21]. MD is widely used to understand the dynamic behavior of proteins, binding stability, and drug-molecule interactions. It is particularly important for providing atomic-level insights into biomolecular systems.

In this work, for the first time a HPLC-MS based methodology, capable to control the remaining concentration of Tryfuzol-neo 1% active substance. These methodologies may be used either for pharmaceutical control, or for veterinary and food probes. The aim of this work also included the methodologies' validation for quantitative and marginal tests for different media. Gaussian calculations were performed to examine Tryfuzol-neo at the B3LYP, HF, and M062X levels [22-24], utilizing the 6-31g, 6-31++g, and 6-31++g(d,p) basis set. The manner and the constructed interactions between Tryfuzol-neo and six cancer-related protein targets were investigated using molecular docking and molecular dynamics simulation. 2JW2 [25], 2H80 [26], and 3WZE [27] were selected for liver cancer. 2XIR [28] and 5C5S [29] were selected for kidney cancer, and 3VF8 [30] was selected for spleen cancer.

2. Computational Method

2.1. Reagents

The piperidinium- $\{[5-(2\text{-furan})-4\text{-phenyl}-4\text{H}-1,2,4\text{-triazole-3-ylthio}]$ acetate (main substance of

Tryfuzol-neo 1%-neo), used as an analyte, with the formula, represented on the Figure 1 ($m/z=302,1$), has been synthesized in our previous work [31]. The acetonitrile "HPLC Super Gradient" has been acquired from Avantor Performance Materials (Poland S.A., Poland). The superpurified water (18 M Ω at 25 °C) was obtained by the system for water purification Direct Q 3UV Millipore (Molsheim, France). The formic acid (100%) has been acquired from (AppliChem GmbH, Germany).

2.2. Apparatus

For chromatographic experiments, the HPLC-MS system: Agilent 1260 Infinity, including degasator, binary pump, autosampler, monoquadruple MS detector Agilent 6120 with the electrospray ionization API-ES) has been used. The interpretation of the spectra was given by the program complex OpenLAB CDS.

2.3. Chromatographic conditions

The analytical chromatographic column Agilent ZORBAX SB-C18 (30 mm x 4,6 mm; 1,8 μm , Agilent Corporation) with the correspondent pre-column has been used. The column temperature was put to 40 °C, the injection volume was fixed to 1 μL . The velocity of the labile phase was equal to 0,4 mL/min in the isocratic conditions. The labile phase was composed of 0,1% (volume) of the formic acid in water, containing 0,1% (volume) of the formic acid (B). The composition of the labile phase was of 70% A/30% B (volume). The experiment lasted 5 minutes.

2.4. MS conditions for the quantitative determination of Tryfuzol-neo 1%-neo 1%

The MS conditions were optimized in order to obtain the maximal output as: 1) the selective ion monitoring (SIM) mode with m/z 302.1 (API Tryfuzol-neo); 2) positive polarity; 3) drying gas (nitrogen) supply velocity - 10 L/min; 4) capillary voltage 4000 V; 5) the drying gas temperature (T), fragmentator voltage (U) and nebulizer pressure (P) are represented in the Table.1.

Volodymyr Parchenko, Alireza Poustforoosh, Yuri Karpenko, Boris Kyrychko, Burak Tüzün, Elena Kyrychko, Tatiana Chetvertak, İlayda Bersu Kul

Table 1. The optimized mass-spectroscopic ionization parameters

The optimized conditions		
T, °C	U, V	P, psi
247	149	46



Figure 2. The sample preparation technique

The preparation of the standard solutions, calibration solutions and the quality-control samples:

1) The initial solution of the active substance of “Tryfuzol-neo 1%-neo 1%” (0,1 mg/ml) (solution A) was prepared in the 100,0 ml beaker by the dissolution of 0,01000 g of the substance in water, diluting the solution till the mark.

2) The preliminary standard solution of the active substance of «Tryfuzol-neo 1%-neo 1%» (0,01 mg/ml) (solution B) was produced by transferring 10,00 ml of the solution A in the 100,0 ml beaker and diluting it till the mark.

3) The final standard solution of the active substance 'Tryfuzol-neo 1%-neo 1%' (0.001 mg/ml) (solution C) was prepared by transferring 10.00 ml of solution A into a 100.0 ml volumetric flask and diluting to the mark with water. In order to produce the model mixtures for determination

in eggs, the homogenate of the eggs has been made by blender.

4) In order to verify the linearity, 7 model solutions with 0 µL, 10 µL, 20 µL, 40 µL, 50 µL, 80 µL, 100 µL were added by the pipet dosator to 0,1000 g to meat or organ homogenate and weighted. Furthermore, 100 µL, 90 µL, 80 µL, 60 µL, 50 µL, 20 µL, 0 µL of water were added correspondently to the above mentioned mixtures. Then the procedure, mentioned in 3 was used in Figure 2.

5) In order to verify the precision and correction, 20 model solutions (5 solutions for 4 concentration levels) have been prepared. For this, the different quantities of the solution C have been added to the 100 mg of the homogenate. The levels chosen were of LLOQ (10 µL), of the three-fold LLOQ (low QC sample)–20 µL (approximately 50% of the calibration curve range) (medium QC) - 50 µL and up to 75 % of the

Volodymyr Parchenko, Alireza Poustforoosh, Yuri Karpenko, Boris Kyrychko, Burak Tüzün, Elena Kyrychko, Tatiana Chetvertak, İlayda Bersu Kul

upper range of the calibration curve (high QC)-80 µL. The solution was weighted and added 90, 80, 50 and 20 µL of water, and the procedure, mentioned in 3 in Figure 2 has been applied.

6) In order to verify the elimination degree of the substance, the non-extracted solutions of active substance of “Tryfuzol-neo 1%-neo” in four concentration levels have been prepared by mixing 10 µL, 20 µL, 50 µL and 80 µL of the solution correspondently with 90 µL, 80 µL, 50 µL and 20 µL of water and 1 ml of methanol.

All the standart solutions were kept by 5 °C and stable during the validation experiment.

2.5. The liquid extraction of the sample

The sample of the eggs were homogenized by blender. 100 µL of the water were added to 0,1000 g of homogenate, stirred by 15 minutes in the ultrasonic bath. Then 1,00 mL of DMSO was added, stirred for 15 minues, centrifuged 15000 G for 10 min and filtered out via a nylon filter (D = 13 mm, pore diameter 0,2 µm). The samples were prepared as on the Figure 2.

The validation of technique

The specificity of the method has been confirmed by analysis of the blank samples in order to determine the absence of the interference of the analyte.

The lower limit of quantification (LLOQ) was determined by the model mixture, which let the five-fold relation between the signal and inferences. The precisiy of this determination wasn't superior to 20%, and the calculated concentration value wasn't superior by more than 20 % of the real analyte concentration in the model mixture.

The lower calibration standard was set according to the LLOQ [32, 33].

The precisiy and correction of the technique were defined by the investigation of the standard samples, prepared according to 5). The elimination degree was determined by the confirmation of the extracted samples by the four levels, estipulated in 6) with the samples, prepared according to 7).

2.6. The application of the remaining quantities of the substance

The remaining quantities of the active substance were realized according to the procedure in the Figure 3, comparing it with the calibration homogenate samples, prepared according to the

calibration samples of homogenate in Figure 2 by adding of the standart solution of the active substance.

The concentration calculation is made according to the calibration equation, which has to be built each time in the experimental conditions.

2.7. Theoretical calculations

A significant amount of information regarding the chemical and biological properties of molecules can be obtained through the use of theoretical calculations. Theoretical computations are used to gather a great deal of information regarding quantum chemical parameters. To provide an explanation for the chemical activities of the molecules, the parameters that were calculated are utilized. To calculate molecules, a wide variety of applications are utilized. Gaussian09 RevD.01 and GaussView 6.0 are the names of these different applications [34,35]. computations were performed at the 6-31++g(d,p) basis set utilizing the B3LYP, HF, and M06-2x [22-24] methods. These programs were utilized to perform the computations. Numerous quantum chemical parameters have been discovered as a consequence of these computations for quantum chemistry. The following is a calculation of the parameters that have been calculated; each parameter describes a different chemical property of molecules. The numbers [36,37].

$$\begin{aligned}\chi &= -\left(\frac{\partial E}{\partial N}\right)_{v(r)} = \frac{1}{2}(I + A) \cong \frac{1}{2}(E_{HOMO} + E_{LUMO}) \\ \eta &= -\left(\frac{\partial^2 E}{\partial N^2}\right)_{v(r)} = \frac{1}{2}(I - A) \cong -\frac{1}{2}(E_{HOMO} - E_{LUMO}) \\ \sigma &= 1/\eta \quad \omega = \chi^2/2\eta \quad \varepsilon = 1/\omega\end{aligned}$$

It is possible to analyze the biological activities of molecules in relation to biological substrates by doing molecular docking simulations. The Maestro Molecular Modeling platform, version 13.4, which was developed by Schrodinger [38], was utilized in order to carry out experiments involving molecular docking of molecules. The process consists of a number of steps, each of which is carried out in detail. During the preliminary phase, the Glide ligand docking module [39,40], the LigPrep module [41], and the protein preparation module [42] were utilized in order to investigate the interactions that occurred between the molecules and the protein after it had been prepared. At every stage of the

Volodymyr Parchenko, Alireza Poustforoosh, Yuri Karpenko, Boris Kyrychko, Burak Tüzün, Elena Kyrychko, Tatiana Chetvertak, İlayda Bersu Kul

calculation process, the OPLS4 approach was utilized. It is planned to conduct an ADME/T study, which stands for absorption, distribution, metabolism, excretion, and toxicity, in order to assess the possible pharmacological effects of the substances that are being investigated. For the purpose of predicting the effects and reactions of substances within the human metabolism, the Qik-prop module [43] of the Schrodinger software was applied.

To assess the robustness of the docking and the interactions between the protein and the ligand, we conducted a molecular dynamics simulation. The molecular dynamics simulation of the ligand-protein complex exhibiting the highest binding affinity was conducted using the Maestro Molecular Modeling platform from Schrödinger, version 12.8 [38]. The OPLS force field was employed to minimize the energy associated with the bond between the ligand and the proteins prior to initiating the molecular dynamics simulation [44,45]. To commence the molecular dynamics simulation, we employed the OPLS force field to minimize the energy linked to the interaction between the ligand and the proteins. The ligand-protein complex was arranged within an orthorhombic box, ensuring a buffer distance of 10 Å to support the modeling of hydration. The system was subsequently neutralized through the addition of suitable amounts of Na⁺ and Cl⁻ ions. The parameters concerning the dimensions, temporal duration, initial temperature, and pressure of the ligand-protein complex were defined as 9 Å, 2.0 fs, 310.15 K (37°C), and 1.01325 bar, respectively, over a duration of 100 ns, in the context of analyzing Van der Waals and electrostatic interactions [46]. A variety of parameters, such as RMSD, defined interactions, and the stability of the secondary structure of the protein, were evaluated.

3. Results and discussion

3.1. Sensitivity (LLOQ determination)

The chromatogram of the meat homogenate without active substance of Tryfuzol-neo 1% (matrix blank) is represented on the Figure 3.

The sound/noise relation for the QC sample in the LLOQ point in Figure 4 was equal to 17,2, which is correspondent to [47,48] (the value needed is ≥5). LLOQ was equal to 0,01 in the weight sample, or 0,1 µg/g (0,1 ppm) of homogenate.

3.2. The identification of the “Tryfuzol-neo 1% neo” active substance and the selectivity

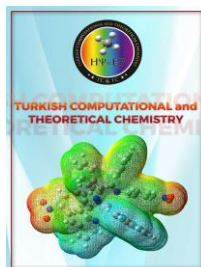
The peak of the “Tryfuzol-neo 1%-neo” active substance was observed in the chromatograms of the model mixtures in LLOQ, and its maintenance time was 3,3-3,5. The MS-detection was carried out in SIM mode with m/z=302,1 being selective, due to its correspondence to the specific monoisotopic quasimolecular protonated ion weight. The interference with the additional components was absent in Figure 3. The chromatographic investigation lasted 4 minutes.

3.3. The linearity of the calibration curve

The calibration curve was built by the dependence of the MS detector output with m/z 302,1 of substance concentration in the homogenate. The calibration was made by use of the external standard. The linearity was observed in the range of 0,012-0,105 µg of weight, or 0,105-0,5 µg/g of homogenate. The linearity was satisfactory, and the equation may be expressed as: $y = 3E+11x + 742,76$, $R^2 = 0,9921$, $R = 0,9960$.

3.4. The precision and the correction of the determination

The content of the active substance of «Tryfuzol-neo 1%-neo» in QC samples was detected by the equation of the calibration curve. The precision and correction of the technique were used for the quality control check. The correction and the precisivity of the data are put in the Table 2.



Received: 17.04.2025

Accepted: 20.05.2025

Research Article

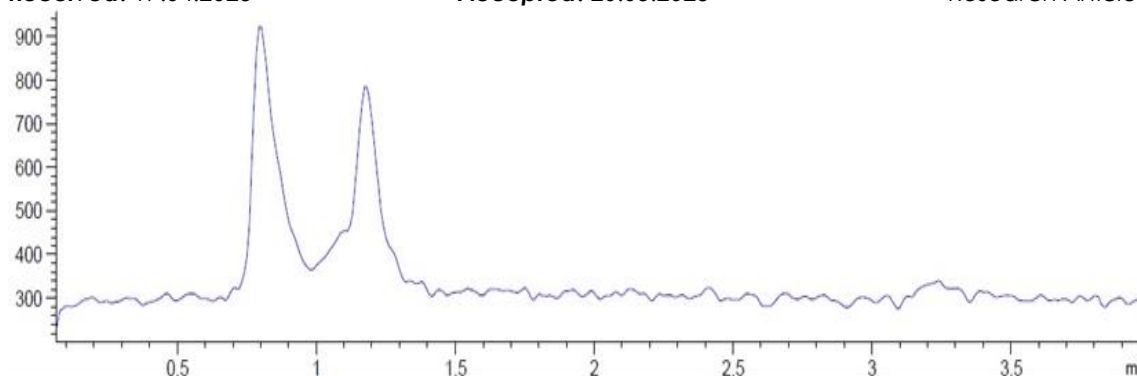


Figure 3. The homogenate chromatogram extract without the active substance (matrix blank)

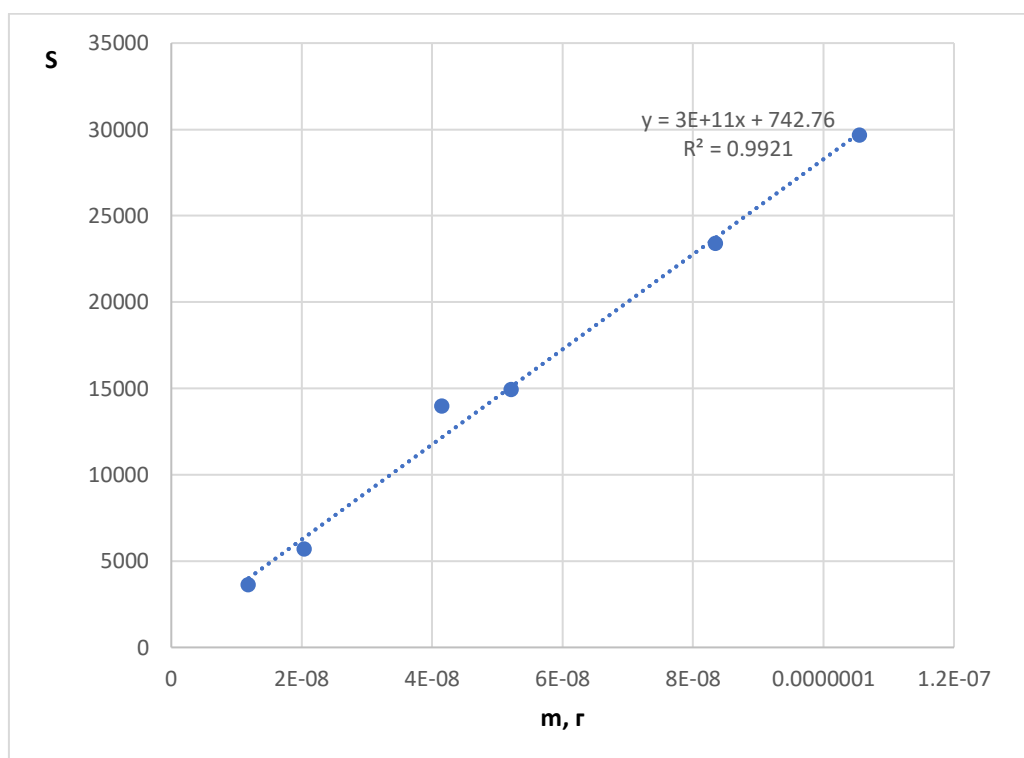


Figure 4. The calibration curve of the dependence of the peak area and the analyte weight in homogenate (g)

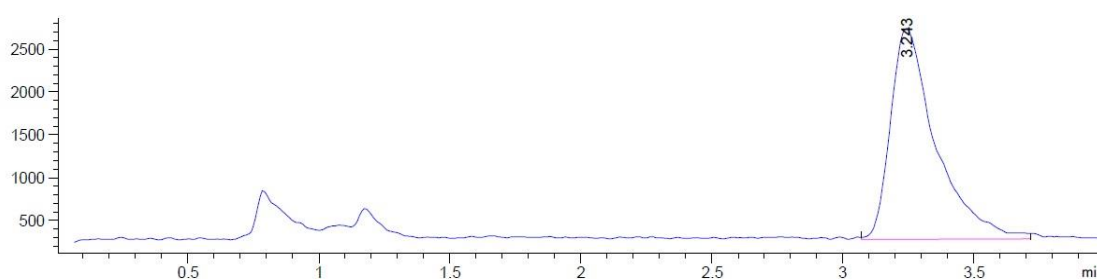


Figure 5. The homogenate chromatogram extract with the active substance (the highest detection limit)

Volodymyr Parchenko, Alireza Poustforoosh, Yuri Karpenko, Boris Kyrychko, Burak Tüzün, Elena Kyrychko, Tatiana Chetvertak, İlayda Bersu Kul

Table 2. The precision and correction of the determination of “Tryfuzol-neo 1%-neo” active substance (n = 5) for 4 concentration levels

Levels	\bar{x} , g In the weight sample	\bar{x} , founjd	Precisity, RSD (%)	Correction, RE (%)	Elimination degree, (%)
1	$8,77 \cdot 10^{-09}$	$7,94 \cdot 10^{-09}$	16,74	-9,45	78,82
2	$2,14 \cdot 10^{-08}$	$2,17 \cdot 10^{-08}$	7,23	1,29	97,49
3	$4,99 \cdot 10^{-08}$	$5,37 \cdot 10^{-08}$	5,56	7,67	96,99
4	$7,98 \cdot 10^{-08}$	$7,10 \cdot 10^{-08}$	14,48	-11,01	94,11

The elimination degree was determined for the solution of quality control check, comparing to the non-extracted comparison solutions with the correspondent active substance concentration. The elimination degree values are represented in the Table 2.

The use of the analytical methodology for the determination of the remaining quantities of the «Tryfuzol-neo 1%» active substance concentration in homogenate.

This technique has manifested its reproducibility, exactity and sensitivity, so it may be efficient for the determination of the remaining quantities of the Tryfuzol-neo 1%-neo active substance. The meat and organ samples (approximate to 0,1 g) are treated as on the Figure 3, and the active substance content is calculated according to the equation of the calibration curve.

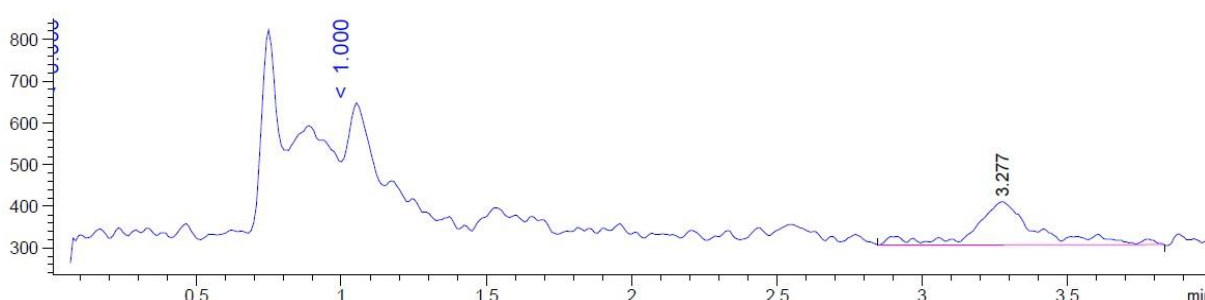


Figure 6. The chromatogram of the extract of the liver homogenate, used in the investigation (after 48 hours)

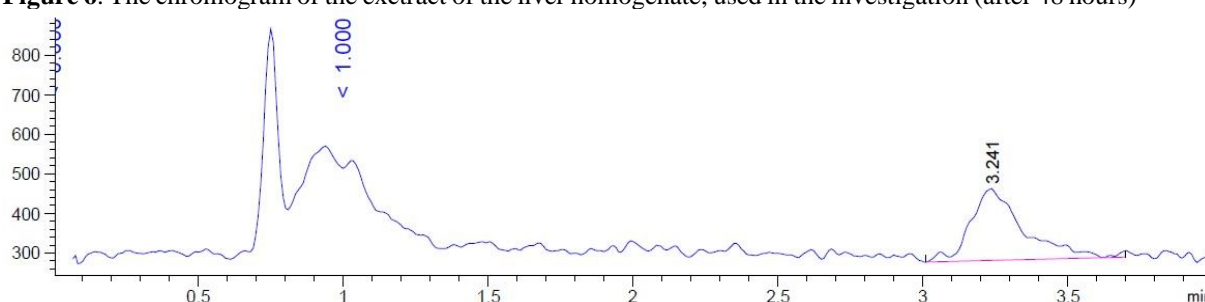


Figure 7. The chromatogram of the extract of the spleen homogenate, used in the investigation (after 48 hours)

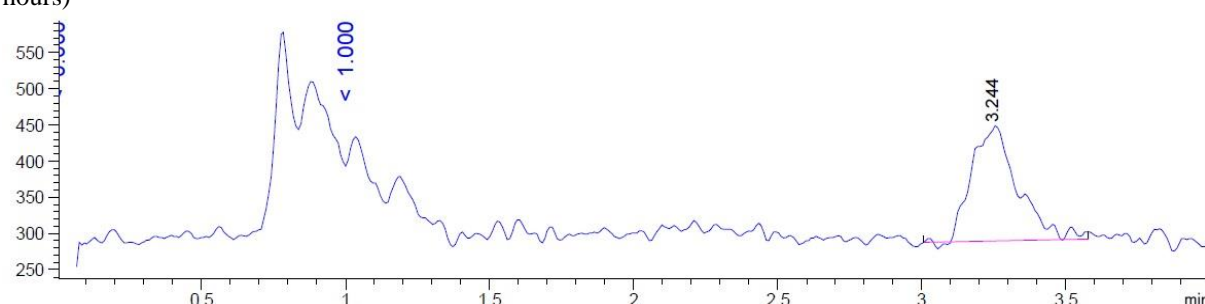


Figure 8. The chromatogram of the extract of the fat tissue homogenate, used in the investigation (after 48 hours)

Volodymyr Parchenko, Alireza Poustforoosh, Yuri Karpenko, Boris Kyrychko, Burak Tüzün,
Elena Kyrychko, Tatiana Chetvertak, İlayda Bersu Kul

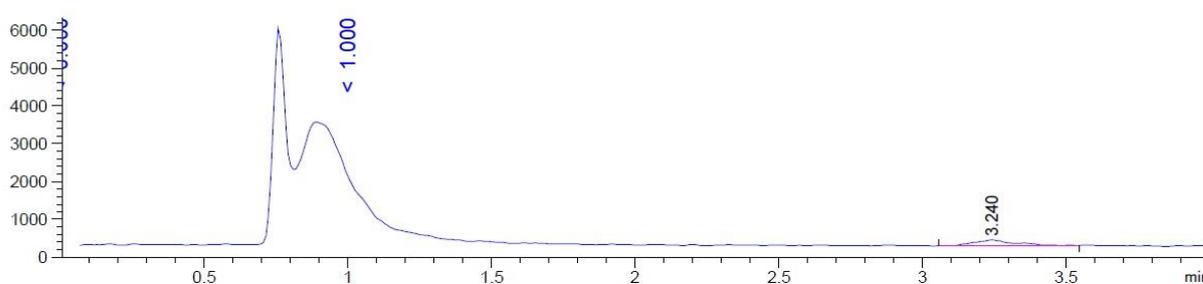


Figure 9. The chromatogram of the extract of the kidney homogenate, used in the investigation (after 48 hours)

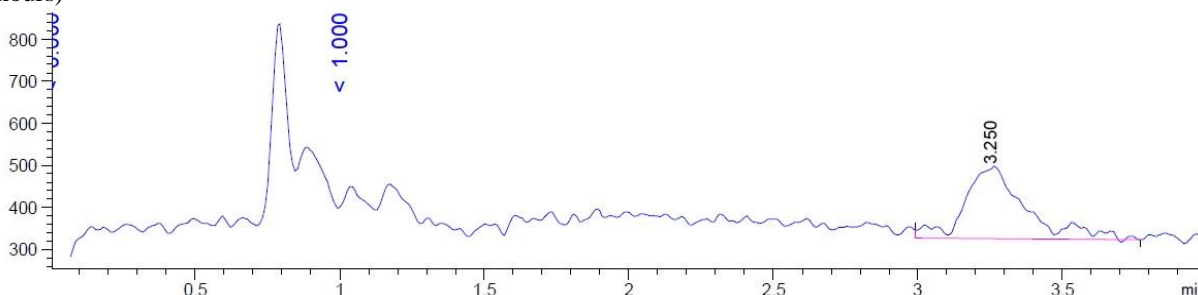


Figure 10. The chromatogram of the extract of the leg muscular tissue homogenate, used in the investigation (after 48 hours)

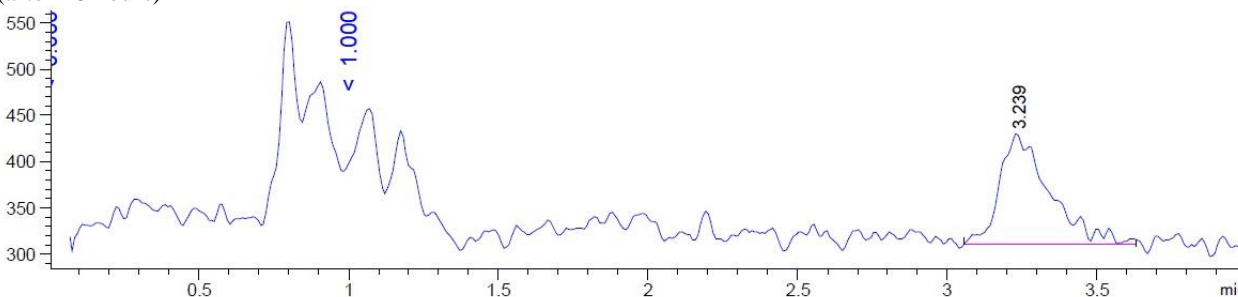


Figure 11. The chromatogram of the extract of the paddle muscular tissue homogenate, used in the investigation (after 48 hours)

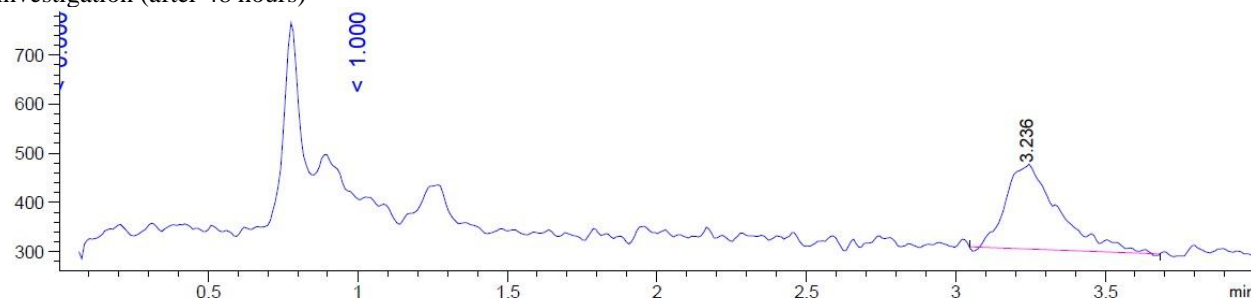


Figure 12. The chromatogram of the extract of the reproductive organs homogenate, used in the investigation (after 48 hours)

Volodymyr Parchenko, Alireza Poustforoosh, Yuri Karpenko, Boris Kyrychko, Burak Tüzün, Elena Kyrychko, Tatiana Chetvertak, İlayda Bersu Kul

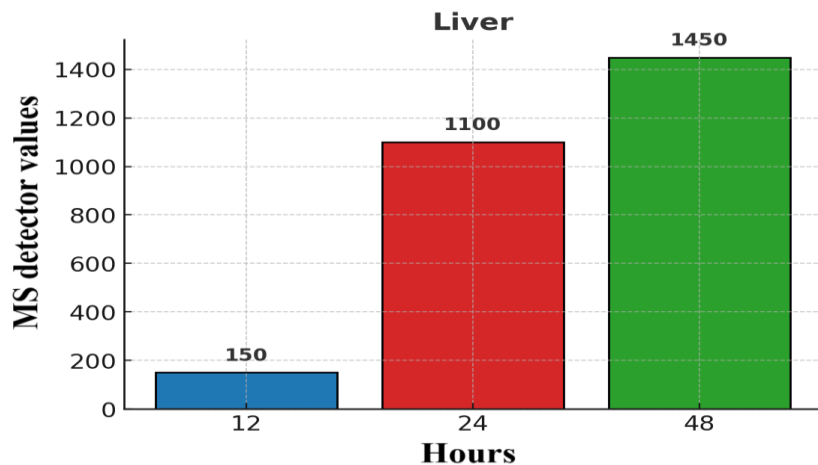


Figure 13. The MS detector values in SIM mode ($m/z=302,1$) for the liver samples after 12, 24 and 48 hours

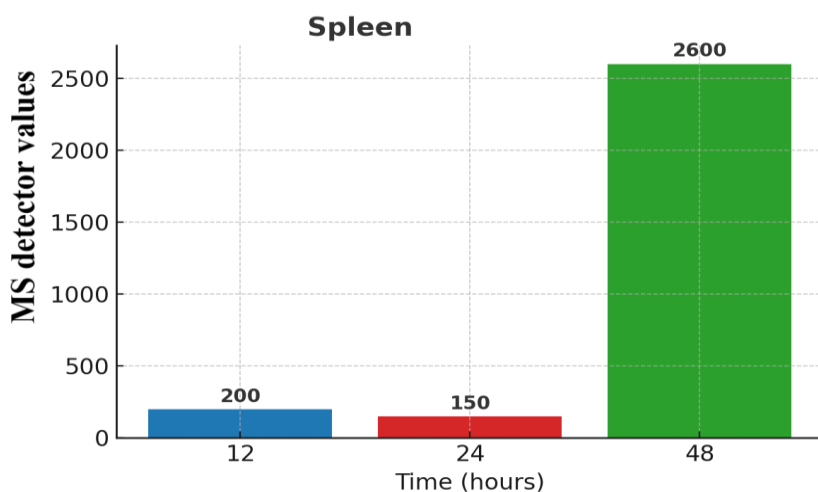


Figure 14. The MS detector values in SIM mode ($m/z=302,1$) for the spleen samples after 12, 24 and 48 hours

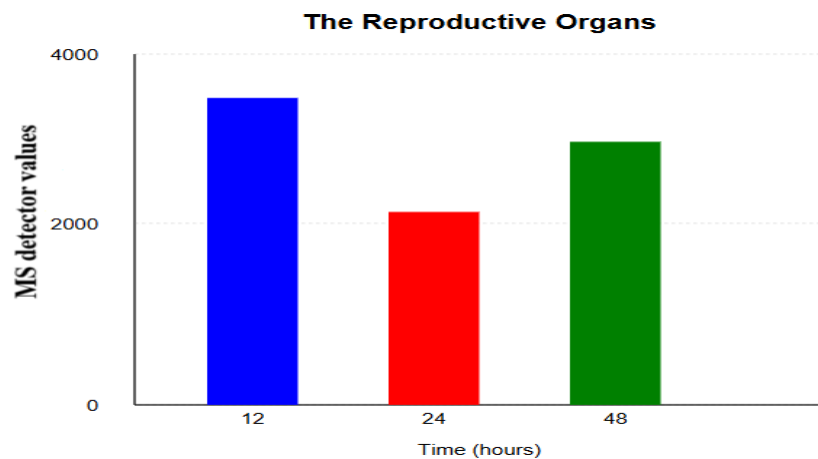


Figure 15. The MS detector values in SIM mode ($m/z=302,1$) for the reproductive organs after 12, 24 and 48 hours

Volodymyr Parchenko, Alireza Poustforoosh, Yuri Karpenko, Boris Kyrychko, Burak Tüzün, Elena Kyrychko, Tatiana Chetvertak, İlayda Bersu Kul

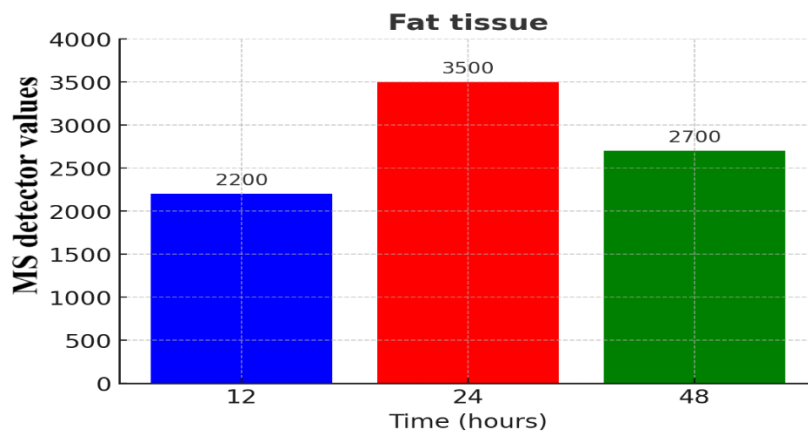


Figure 16. The MS detector values in SIM mode ($m/z=302,1$) for the fat tissue samples after 12, 24 and 48 hours

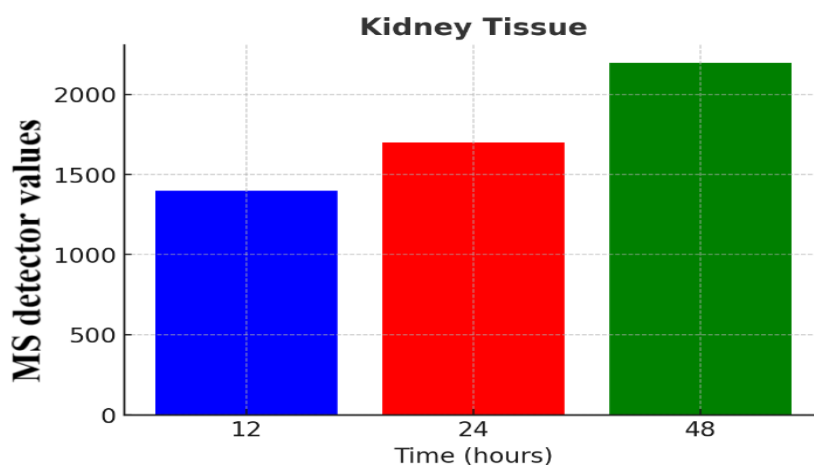


Figure 17. The MS detector values in SIM mode ($m/z=302,1$) for the kidney samples after 12, 24 and 48 hours

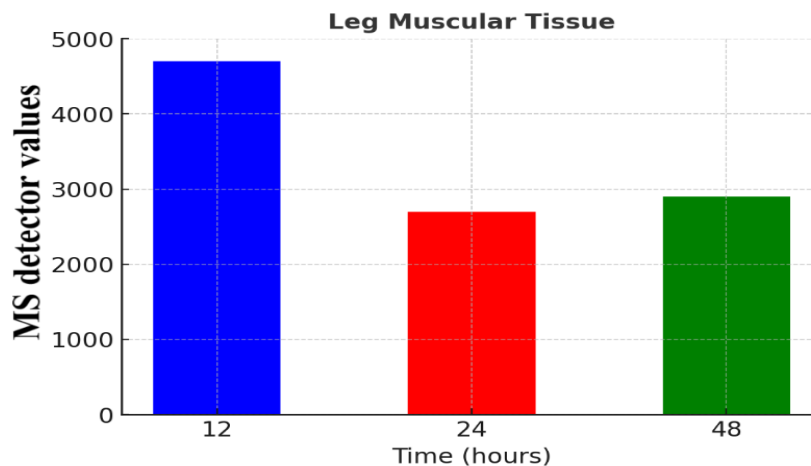


Figure 18. The MS detector values in SIM mode ($m/z=302,1$) for the leg muscular tissue samples after 12, 24 and 48 hours

Volodymyr Parchenko, Alireza Poustforoosh, Yuri Karpenko, Boris Kyrychko, Burak Tüzün, Elena Kyrychko, Tatiana Chetvertak, İlayda Bersu Kul

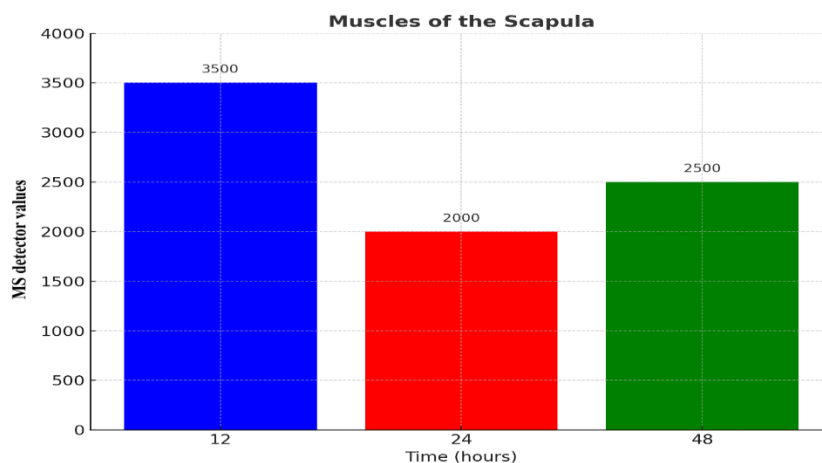


Figure 19. The MS detector values in SIM mode ($m/z=302,1$) for the puddle muscular tissue samples after 12, 24 and 48 hours

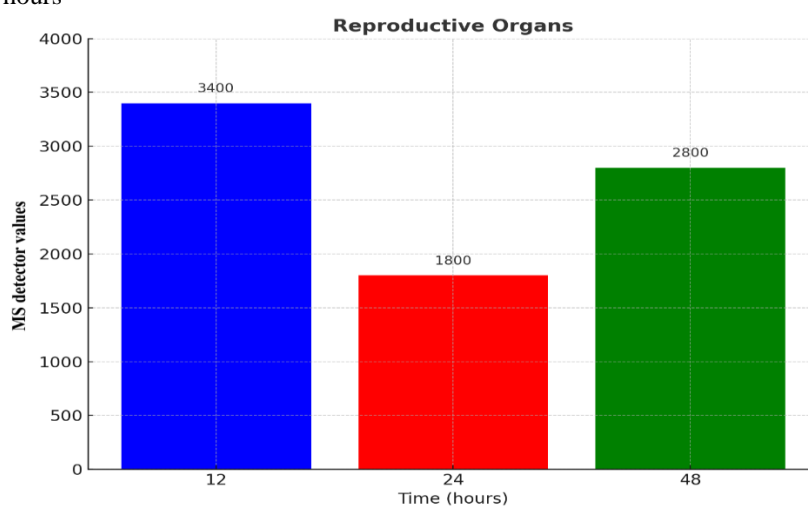


Figure 20. The MS detector values in SIM mode ($m/z=302,1$) for the reproductive organs after 12, 24 and 48 hours

The chromatogram of the extract are given in the Figure 6-12. The MS detector values are given in Figure 13-20. The analysis of the results of the detection of the presence of the “Tryfuzol-neo 1%-

neo” active substance after 72 hours confirms the absence of this active substance in the investigated organ samples and in meet. The correspondent chromatograms are exposed in the Figure 21–27.

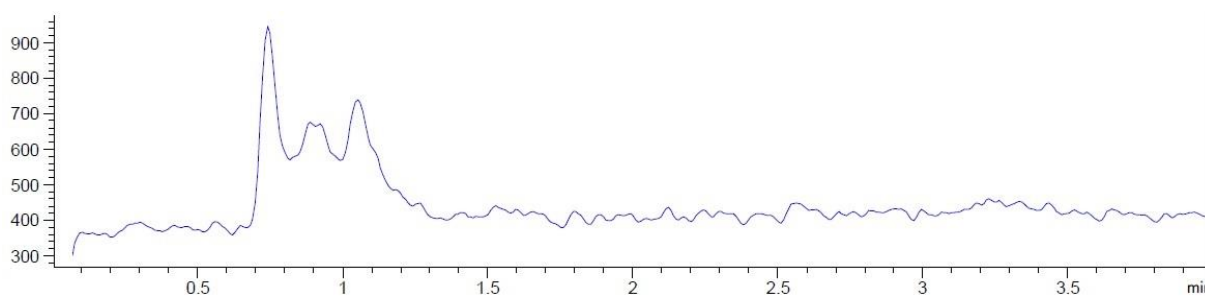


Figure 21. The chromatogram of the extract of the liver homogenate, used in the investigation (after 72 hours)

Volodymyr Parchenko, Alireza Poustforoosh, Yuri Karpenko, Boris Kyrychko, Burak Tüzün,
Elena Kyrychko, Tatiana Chetvertak, İlayda Bersu Kul

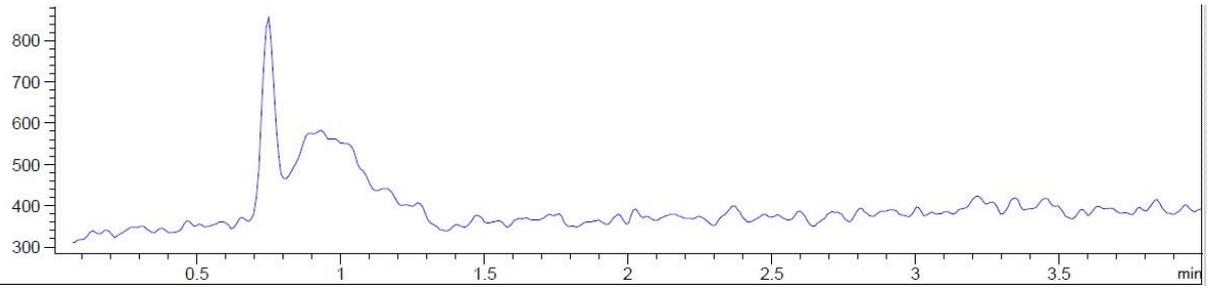


Figure 22. The chromatogram of the extract of the spleen homogenate, used in the investigation (after 72 hours)

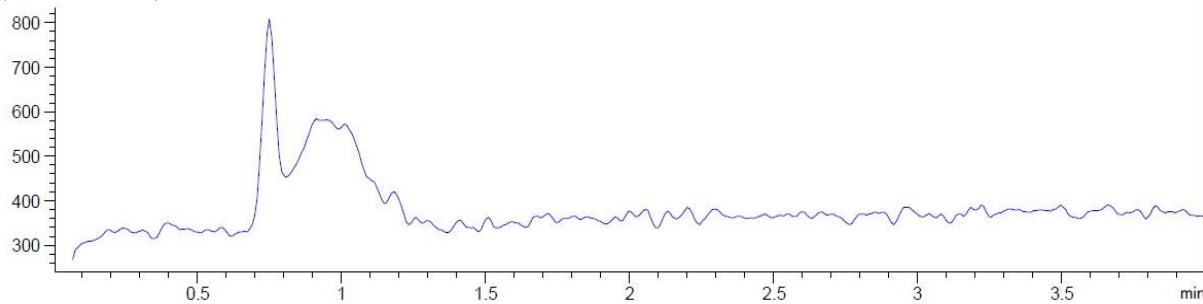


Figure 23. The chromatogram of the extract of the fat tissue homogenate, used in the investigation (after 72 hours)

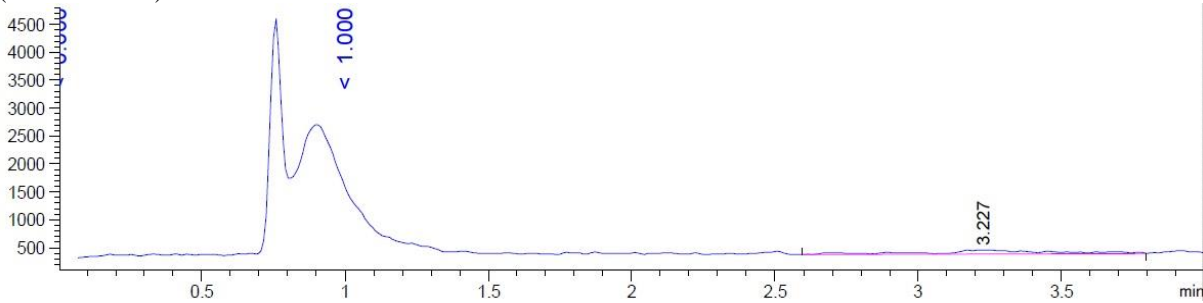


Figure 24. The chromatogram of the extract of the kidney homogenate, used in the investigation (after 72 hours)

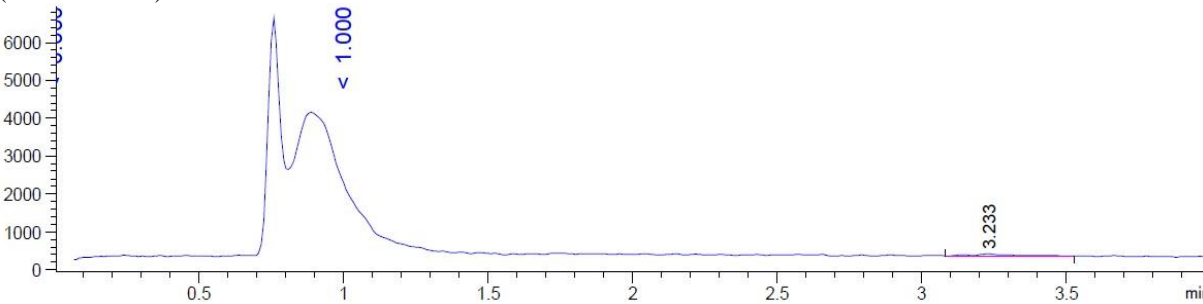


Figure 25. The chromatogram of the extract of the leg muscular tissue homogenate, used in the investigation (after 72 hours)

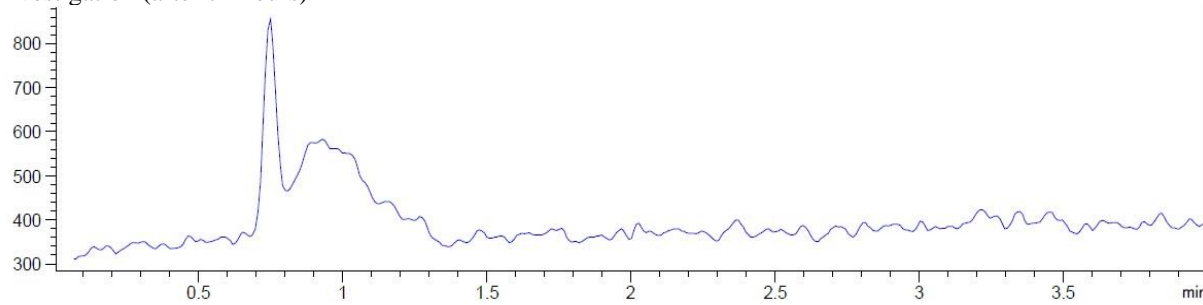


Figure 26. The chromatogram of the extract of the puddle muscle tissue homogenate, used in the investigation (after 72 hours)

Volodymyr Parchenko, Alireza Poustforoosh, Yuri Karpenko, Boris Kyrychko, Burak Tüzün, Elena Kyrychko, Tatiana Chetvertak, İlayda Bersu Kul

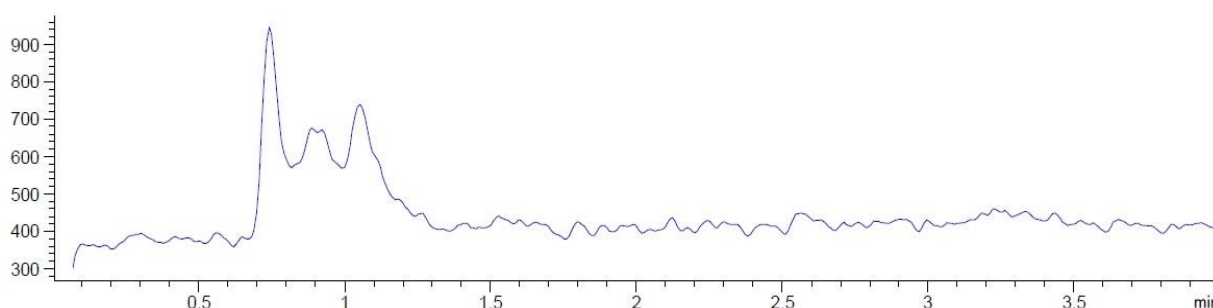


Figure 27. The chromatogram of the extract of the reproductive organ homogenate, used in the investigation (after 72 hours)

Table 3. The results of the “Tryfuzol-neo 1%” active substance determination in control groups

Organ		Hours	12	24	48	72
Liver	m, mkg		None**	Detected*	Detected*	None**
	C, µg/g		None**	Detected*	Detected*	None**
Spleen	m, mkg		None**	None**	Detected*	None**
	C, µg/g		None****	None**	Detected*	None**
Fat tissue	m, mkg		Detected*	Detected*	Detected*	None**
	C, µg/g		Detected*	Detected*	Detected*	None**
Kidney	m, mkg		Detected*	Detected*	Detected*	None**
	C, µg/g		Detected*	Detected*	Detected*	None**
Leg muscular tissue	m, mkg		0,01224	Detected*	Detected*	None**
	C, µg/g		0,1045	Detected*	Detected*	None**
Puddle muscular tissue	m, mkg		Detected*	Detected*	Detected*	None**
	C, µg/g		Detected*	Detected*	Detected*	None**
Reproductive organs	m, mkg		Detected*	Detected*	Detected*	None**
	C, µg/g		Detected*	Detected*	Detected*	None**

*Detected, but the concentration is below the detection limit ($c < 0,1$ ppm), **Not detected

Table 4. The calculated quantum chemical parameters of molecules.

	E _{HOMO}	E _{LUMO}	I	A	ΔE	η	μ	χ	PA	ω	ε	dipol	Energy
B3LYP/6-31g LEVEL													
	-4.3571	-0.2378	4.3571	0.2378	4.1193	2.0596	0.4855	2.2975	-2.2975	1.2814	0.7804	8.847	-42105.4290
B3LYP/6-31++g LEVEL													
	-4.6129	-0.7470	4.6129	0.7470	3.8660	1.9330	0.5173	2.6799	-2.6799	1.8578	0.5383	9.446	-42106.7112
B3LYP/6-31++g(d,p) LEVEL													
	-4.7843	-0.8632	4.7843	0.8632	3.9212	1.9606	0.5100	2.8237	-2.8237	2.0335	0.4918	5.049	-42117.2893
HF/6-31g LEVEL													
	-6.5066	3.7362	6.5066	-3.7362	10.2427	5.1214	0.1953	1.3852	-1.3852	0.1873	5.3381	9.296	-41886.1469
HF/6-31++g LEVEL													
	-6.6560	0.7138	6.6560	-0.7138	7.3697	3.6849	0.2714	2.9711	-2.9711	1.1978	0.8349	9.654	-41887.0547
HF/6-31++g(d,p) LEVEL													
	-6.4285	0.6906	6.4285	-0.6906	7.1191	3.5595	0.2809	2.8689	-2.8689	1.1561	0.8649	10.014	-41902.0712
M062X/6-31g LEVEL													
	-6.3517	0.2814	6.3517	-0.2814	6.6331	3.3165	0.3015	3.0352	-3.0352	1.3888	0.7200	5.248	-42091.8208
M062X/6-31++g LEVEL													
	-5.9376	-0.4057	5.9376	0.4057	5.5318	2.7659	0.3615	3.1716	-3.1716	1.8184	0.5499	7.467	-42092.7412
M062X/6-31++g(d,p) LEVEL													
	-5.9830	-0.2305	5.9830	0.2305	5.7525	2.8763	0.3477	3.1067	-3.1067	1.6778	0.5960	4.794	-42102.7810

Table 5. Numerical values of the docking parameters of tryfuzol against the proteins related to various cancer, such as liver, kidney, and spleen.

Volodymyr Parchenko, Alireza Poustforoosh, Yuri Karpenko, Boris Kyrychko, Burak Tüzün, Elena Kyrychko, Tatiana Chetvertak, İlayda Bersu Kul

	Docking Score	Glide ligand efficiency	Glide hbond	Glide evdw	Glide ecoul	Glide emodel	Glide energy	Glide einternal	Glide posenum
2H80	-1.296	-0.062	-0.350	-16.421	-5.361	-24.133	-21.782	2.108	1
2JW2	-2.935	-0.140	-1.138	-20.237	-9.958	-36.414	-30.194	1.793	8
2XIR	-4.449	-0.212	0.000	-24.715	-4.135	-36.942	-28.850	1.518	2
3VF8	-5.145	-0.245	-0.350	-30.315	-3.956	-43.664	-34.271	1.343	7
3WZE	-5.172	-0.246	-0.138	-35.314	-0.731	-46.622	-36.046	1.943	1
5C5S	-2.576	-0.123	-0.629	-23.730	-1.422	-27.280	-25.152	5.944	1

3.5. Theoretical calculations

The Gaussian package program is a widely used software for quantum chemical calculations and offers various theoretical methods for determining the electronic structure of molecular systems. This program allows the calculation of energy levels, electron densities and many parameters related to reactivity of molecules, especially using computational methods such as density functional theory (DFT) and Hartree-Fock (HF). Some important quantum chemical parameters that can be calculated using Gaussian include HOMO (Highest Occupied Molecular Orbital) and LUMO (Lowest Unoccupied Molecular Orbital) [49]. HOMO is the level in which electrons are in the highest energy occupied orbital in a molecule. This orbital determines the electron donor capacity of the molecule [50]. The higher the HOMO energy, the easier the molecule can donate electrons and the higher its reactivity. It is an important parameter especially in organic semiconductors, redox reactions and biological systems. LUMO is the lowest energy empty orbital in the molecule that electrons can pass through [51]. LUMO energy determines the ability of the molecule to accept

electrons. A low LUMO energy makes it easier for the molecule to be an electron acceptor [52]. Electron transfer plays a critical role in chemical reactivity and molecular interactions. All parameters are given in Table 4 and Figure 28 and 29.

The energy difference between HOMO and LUMO is an important parameter that determines the chemical stability and reactivity of the molecule. If this difference is small, the molecule is more reactive and can easily transfer electrons [50]. A large energy difference indicates more stable and less reactive systems. HOMO and LUMO energy levels are also related to ionization potential (IP) and electron affinity (EA). Ionization potential is the energy required to remove an electron from a molecule and is approximately related to the HOMO energy [52]. Electron affinity is the energy change required for the molecule to gain an electron and form an anion and is related to the LUMO energy.

Another important parameter, electronegativity, defines the ability of a molecule to attract electrons and can be calculated by averaging the HOMO and LUMO energies.

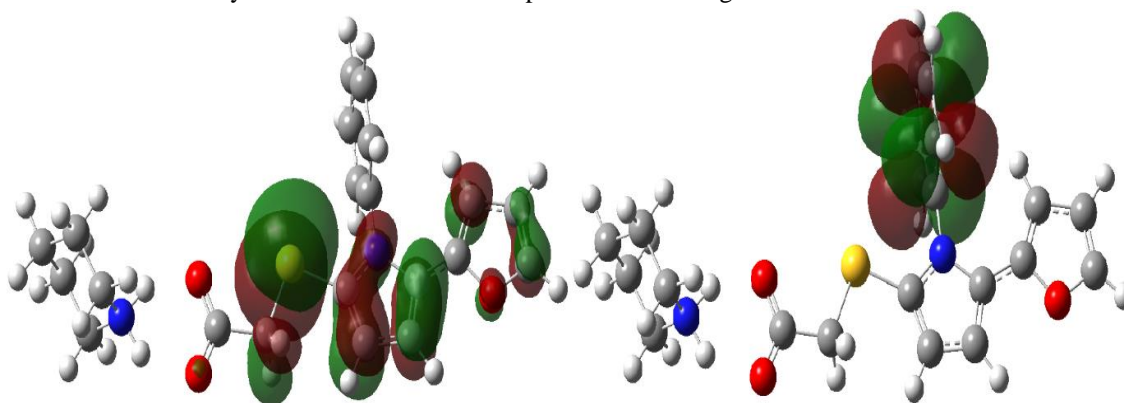


Figure 28. Representation of HOMO and LUMO of molecule.

Volodymyr Parchenko, Alireza Poustforoosh, Yuri Karpenko, Boris Kyrychko, Burak Tüzün, Elena Kyrychko, Tatiana Chetvertak, İlayda Bersu Kul

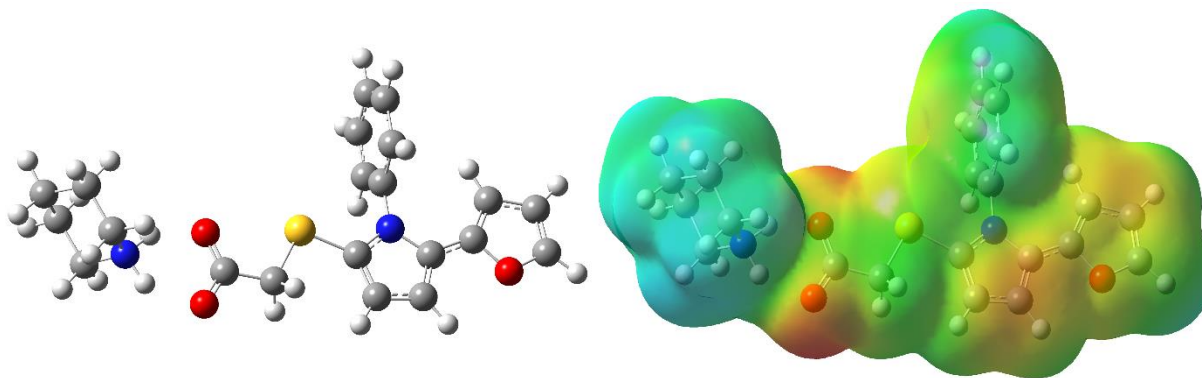
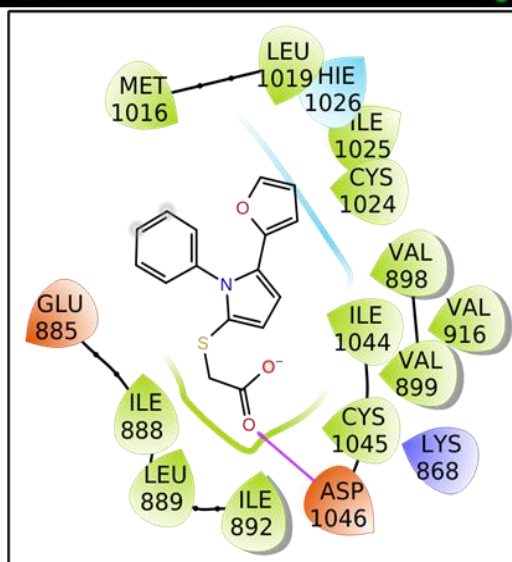


Figure 29. Representation of optimize structure and ESP of molecule



- | | | | |
|--|---|--|--|
| ● Charged (negative) | ● Polar | --- Distance | —●— Pi-cation |
| ● Charged (positive) | ● Unspecified residue | —●— H-bond | —●— Salt bridge |
| ● Glycine | ● Water | —●— Halogen bond | ○ Solvent exposure |
| ● Hydrophobic | ○ Hydration site | —●— Metal coordination | |
| ● Metal | ✗ Hydration site (displaced) | —●— Pi-Pi stacking | |

Figure 30. The docking pose and constructed interactions of Tryfuzol in the active site of KDR (3WZE). There is one hydrogen bond between the compound and Asp1046 and there are also twelve hydrophobic contacts.

Volodymyr Parchenko, Alireza Poustforoosh, Yuri Karpenko, Boris Kyrychko, Burak Tüzün, Elena Kyrychko, Tatiana Chetvertak, İlayda Bersu Kul

Chemical hardness, on the other hand, expresses the resistance of a system to energy changes and is calculated as half of the HOMO-LUMO difference [53]. A high hardness value indicates a more stable molecule, while a low hardness value indicates that the molecule is more reactive.

Chemical potential determines the tendency of a molecule to give and take electrons and is calculated by averaging the HOMO and LUMO energies. Electrophilicity index is a parameter that defines the tendency of a molecule to take electrons and is obtained by dividing the square of the chemical potential by twice the chemical hardness [54]. Molecules with high electrophilicity are more likely to accept electrons.

These parameters are calculated with the Gaussian program and provide information about the chemical reactivity of molecular systems, their biological activity, material science applications and potential uses in catalytic processes. HOMO and LUMO energies, in particular, are of critical importance in many areas such as drug design, organic semiconductors and sensor technologies. Calculations may be utilized to evaluate the interactions of molecules in the presence of biological substances [55]. Anticipating the efficacy of molecules before experimental trials allows for the optimization of their characteristics prior to testing. Molecular docking is a widely employed technique for evaluating biological activity. Understanding the interactions of molecules in molecular docking simulations requires that they engage with the protein in a manner consistent with the key-lock model [56,57]. The main determinants of molecular activity are their interactions. Nevertheless, an increase in the frequency of these interactions has been associated with a notable enhancement in the molecules' activity against proteins, as observed by researchers. Various forms of interactions encompass hydrogen bonds, polar interactions, hydrophobic interactions, and π - π interactions [58-60]. The results of the calculations illustrate the properties of molecular interactions concerning proteins associated with cancer. These characteristics are detailed in Table 5 and illustrated in Figure 30.

The performance of fundamental calculations reveals that a significant amount of data is acquired

by analyzing the interactions between molecules and enzymes. The docking score stands out as a significant measure of the functional potential of molecules among these various factors. The docking scores obtained for 3WZE and 3VF8 are -5.172 and -5.145, respectively. This observation indicates that the molecule demonstrates a higher binding affinity for 3WZE relative to the other proteins analyzed. The metrics obtained from Glide hbond, Glide evdw, and Glide ecol are essential for comprehending the interactions that occur between the molecule and the protein [61]. The glide hydrogen bond parameter shows how strong the hydrogen bonds are between molecules and proteins. The protein 3WZE forms a hydrogen bond with the molecule, which has a numerical value of -0.138, creating an attractive force between them. The 3WZE protein connects with the molecule using a Van der Waals force. The number linked to this interaction is -35.314. The glide ecol parameter measures the number of Coulombic interactions happening between molecules and proteins, represented as a numerical value. The Coulombic interaction between the protein 1A3N and the molecule is defined by a numerical value of -0.731. Nevertheless, important factors such as Glide emodel, Glide energy, and Glide einternal offer crucial understanding of the connections between the molecule and the protein. The examination of how tryfuzol and the 3WZE protein interact shows, as shown in Figure 30, the creation of a hydrogen bond between Asp1046 of the protein and the tryfuzol molecule. Furthermore, the compound also shows twelve hydrophobic interactions with Ile888, Leu889, Ile892, Cys1045, Ile1044, Val899, Val898, Val916, Cys1024, Ile1025, Leu1019, and Met1016 residues.

In molecular docking studies, receptor proteins are seen as fixed and unmoving entities, while ligand molecules display flexibility and dynamism when interacting with the receptor. The receptor protein needs to be flexible in order to accurately predict how a drug will interact with it, including the thermodynamic and kinetic factors.

To examine the stability, dynamics, and structural changes of the protein complex being studied, we ran molecular dynamics (MD) simulations spanning 100 nanoseconds. In this situation, we looked at the root mean square deviation (RMSD)

Volodymyr Parchenko, Alireza Poustforoosh, Yuri Karpenko, Boris Kyrychko, Burak Tüzün, Elena Kyrychko, Tatiana Chetvertak, İlayda Bersu Kul

along with a visual representation showing the connections between the ligand and the amino acids. Additionally, we examined the changes in the secondary structure of the protein, which are illustrated in Figure 34. The stability of the complex was assessed by determining its RMSD. RMSD

gives information about the structural shape during the simulation [62]. During the simulation, this calculation measures the average difference in the positions of the $C\alpha$ backbones from the beginning to the end.

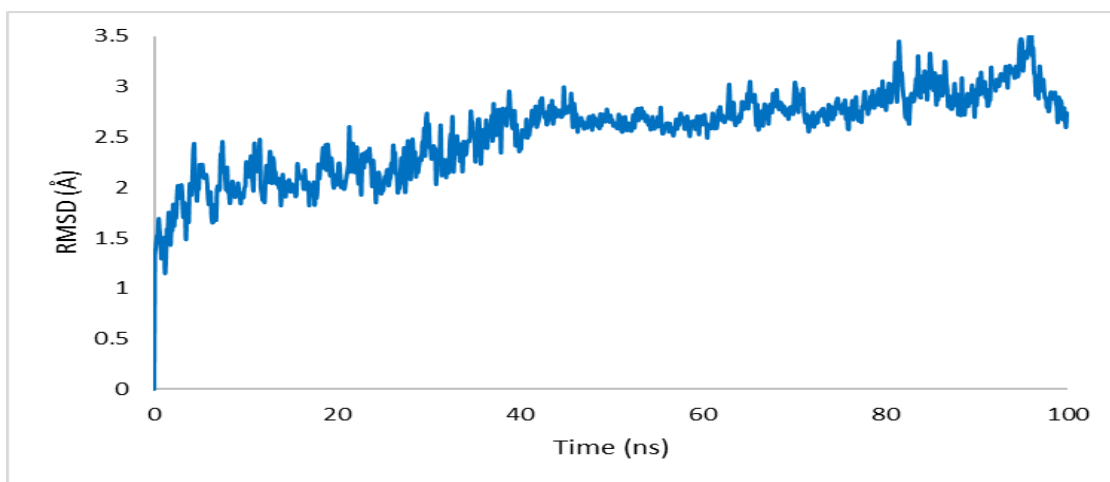


Figure 31. The RMSD values of the hemoglobin during 100 ns, which is equilibrated at about 2.5Å.

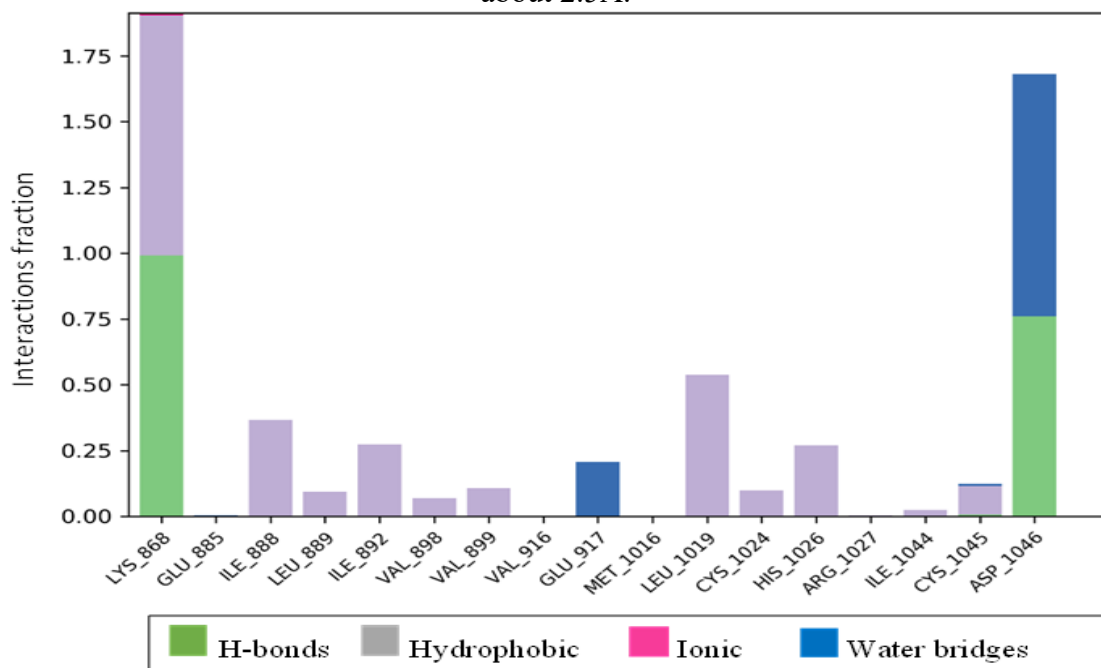


Figure 32. The interactions constructed between Tryfuzol and KDR (3WZE) during the MD simulation. The residues with the highest interaction fraction are Lys868 and Asp1046. Lys868 has formed hydrogen bonds and hydrophobic contacts with the ligand, while these interactions for Asp1046 are hydrogen bond and water bridge.

Figure 32 shows the RMSD value, suggesting that the protein has reached a stable balance around 2.5 Å. Hydrogen bonds formed between a ligand molecule and the protein at the active site aid in the

protein's ability to recognize the ligand. However, the compound cannot interact with any other protein in the same way. Figure 33 demonstrates the interactions formed between tryfuzol and KDR

Volodymyr Parchenko, Alireza Poustforoosh, Yuri Karpenko, Boris Kyrychko, Burak Tüzün, Elena Kyrychko, Tatiana Chetvertak, İlayda Bersu Kul

(3WZE). Lys868 and Asp1046 are the residues that have the highest interaction fraction. During most of the simulation, Lys868 has been involved in hydrogen bonds and hydrophobic contacts with the ligand, whereas Asp1046 has mainly been engaged in hydrogen bonding and forming a water bridge with the ligand. During the simulation, a comprehensive assessment was conducted to inspect the alterations happening in the protein's secondary configuration. Figure 34 shows the

changes in the 3WZE's secondary structure elements (SSE) due to the presence of tryfuzol. The findings from the molecular dynamics simulation show that the protein remains stable, as shown by the small changes observed in the percentage of SSE. The simulation findings consistently show that the proportion of SSE remains steady at approximately 41%.

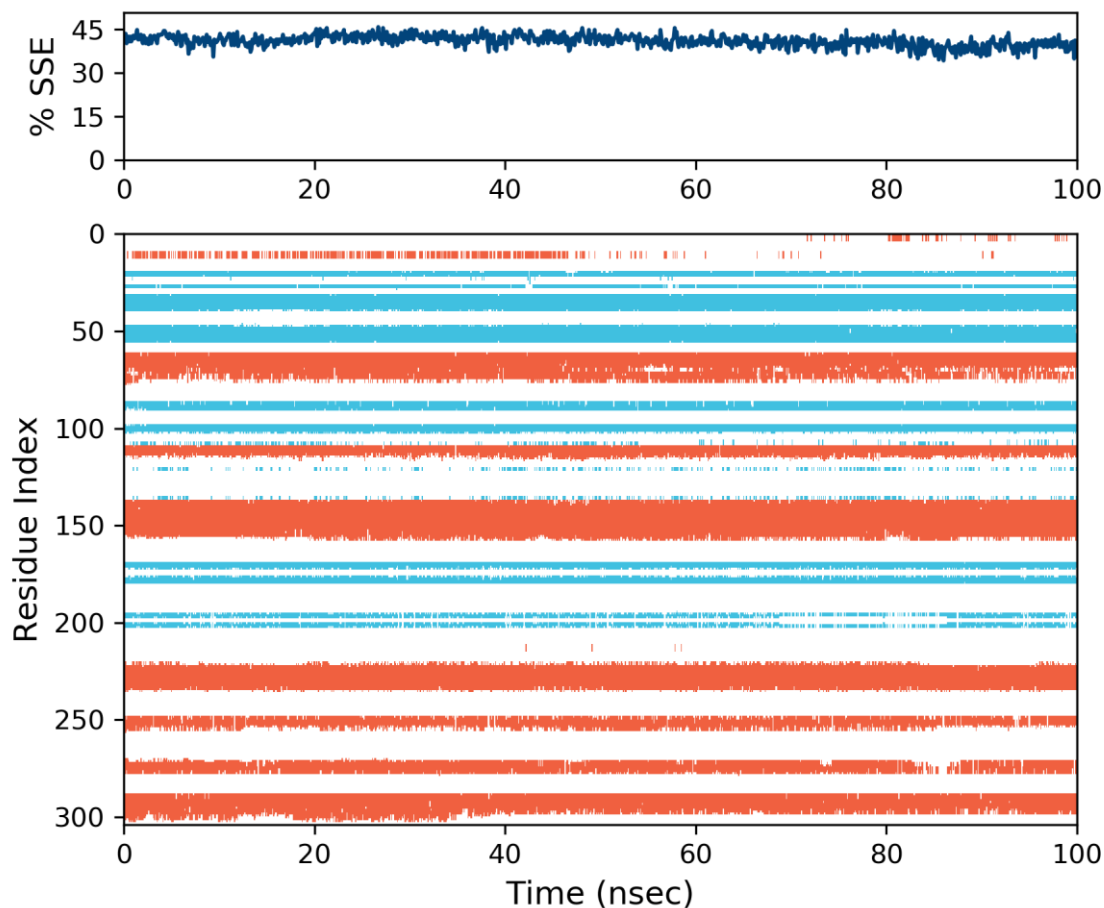


Figure 34. The changes of the secondary structure of KDR (3WZE) throughout the simulation in the presence of Tryfuzol. The percent of SSE has remained at about 41% during the simulation. The red and blue regions indicate the alpha-helices and beta-strands, respectively.

4. Conclusions

In this study, a novel HPLC-MS analytical method was successfully developed for the quantification of the newly formulated drug Tryfuzol-neo 1%, demonstrating its practical applicability in both food safety assessments and veterinary research. The method enabled the detection and quantification of residue levels in meat and various animal organ tissues, underscoring its reliability for

routine analysis. Furthermore, the quantum chemical characteristics of Tryfuzol-neo were comprehensively evaluated through Gaussian-based theoretical calculations at multiple computational levels, providing valuable insights into its molecular structure and reactivity. Complementary to these findings, molecular docking and molecular dynamics simulations were employed to explore the interactions of Tryfuzol-

Volodymyr Parchenko, Alireza Poustforoosh, Yuri Karpenko, Boris Kyrychko, Burak Tüzün, Elena Kyrychko, Tatiana Chetvertak, İlayda Bersu Kul

neo with key protein targets associated with liver, kidney, and spleen cancers. The obtained results elucidate the drug's potential binding mechanisms and biological activity, thereby laying a foundational framework for future pharmacokinetic and pharmacodynamic investigations.

Acknowledgments

Funding Declaration

The numerical calculations reported in this paper were fully/partially performed at TUBITAK ULAKBIM, High Performance and Grid Computing Center (TRUBA resources). This work was supported by the Scientific Research Project Fund of Sivas Cumhuriyet University (CUBAP) under the project number RGD-020.

Conflicts of Interest

The authors declare no competing financial interest or personal relationships.

References

- [1] J.K. Shneine, & Y.H. Alaraji, *Int. J. Recent. Sci. Res.*, (5) (2016) 1411.
- [2] S.B.S. Ganguly, & K.K. Sen, *A Review on 1, 2, 4-Triazoles. Journal of Advanced Pharmacy Education and Research*, 3(3-2013) (2013) 102-115.
- [3] R.K. Singla, & G.V. Bhat, *QSAR model for predicting the fungicidal action of 1, 2, 4-triazole derivatives against Candida albicans. Journal of Enzyme Inhibition and Medicinal Chemistry*, 25(5) (2010) 696-701.
- [4] http://shodhganga.inflibnet.ac.in/bitstream/10603/122880/6/06_chapter%201.pdf, accessed at the 7th of October 2018
- [5] M.S. Saini, & J. Dwivedi, *Synthesis and biological significances of 1, 2, 4-triazole and its derivatives: A review. International Journal of Pharmaceutical Sciences and Research*, 4(8) (2013) 2866.
- [6] A. Martin, & R. Martin, *A review on the antimicrobial activity of 1, 2, 4-triazole derivatives. Int. J. Life Sci. Pharm. Res.*, 3 (2014) 321-329.
- [7] S. Maddila, R. Pagadala, & S.B. Jonnalagadda, *1, 2, 4-Triazoles: A review of synthetic approaches and the biological activity. Letters in Organic Chemistry*, 10(10) (2013) 693-714.
- [8] A.H. Malani, A.H. Makwana, & H.R. Makwana, *A brief review article: Various synthesis and therapeutic importance of 1, 2, 4-triazole and its derivatives. Moroccan Journal of Chemistry*, 5(1) (2017) 41-58.
- [9] N. Singla, J. Bariwal, & S. Kaur, *Design and synthesis of 1, 2, 4-triazole substituted thiophenes. Int J Pharmaceut Sci Res.*, 9 (2018) 158-164.
- [10] V. Borys, K. Andriy, & P. Vladymyr, *Electrospray ionization mass spectrometry fragmentation pathways of salts of some 1, 2, 4-triazolythioacetate acids, the active pharmaceutical ingredients. Asian J Pharm Clin Res.*, 11(10) (2018) 303-312.
- [11] S. Eswaran, A.V. Adhikari, & N.S. Shetty, *Synthesis and antimicrobial activities of novel quinoline derivatives carrying 1, 2, 4-triazole moiety. European journal of medicinal chemistry*, 44(11) (2009) 4637-4647.
- [12] S.K. Reddy, M.N. Purohit, & G.V. Pujar, *Synthesis and pharmacological activity of some novel bis-heterocycles encompassing pyrrole. Int J Pharm Pharm Sci*, 4(5) (2012) 153-157.
- [13] S. Philip, M.N. Purohit, K.K. La, M.S. Eswar, T. Raizaday, S. Prudhvi, G.V. Pujar, *Design, synthesis and in vitro anti-cancer activity of novel 1,2,4-triazole derivatives. Int J Pharm Pharm Sci*, 6(10) (2011) 185-189.
- [14] N.N. Gülerman, H.N. Doğan, S. Rollas, C. Johansson, & C. Celik, *Synthesis and structure elucidation of some new thioether derivatives of 1, 2, 4-triazoline-3-thiones and their antimicrobial activities. Il Farmaco*, 56(12) (2001) 953-958.
- [15] H.A. El-Sherief, B.G. Youssif, S.N.A., Bukhari, M. Abdel-Aziz, & H.M. Abdel-Rahman, *Novel 1, 2, 4-triazole derivatives as potential anticancer agents: Design, synthesis, molecular docking and mechanistic studies. Bioorganic chemistry*, 76 (2018) 314-325.
- [16] I. Bushueva, V. Parchenko, R. Shcherbyna, A. Safonov, A. Kaplaushenko, B. Gutyj, & I. Hariv, *Tryfuzol-new original veterinary drug.*

Volodymyr Parchenko, Alireza Poustforoosh, Yuri Karpenko, Boris Kyrychko, Burak Tüzün, Elena Kyrychko, Tatiana Chetvertak, İlayda Bersu Kul

- Journal of Faculty of Parmak of Ankara University, 41(1) (2017).
- [17] B. Tüzün, Examination of anti-oxidant properties and molecular docking parameters of some compounds in human body. *Turkish Computational and Theoretical Chemistry*, 4(2) (2020) 76-87.
- [18] H. Saraç, , A. Demirbaş, & B. Tüzün, Could Zingiber officinale plant be effective against Omicron BA. 2.75 of SARS-CoV-2?. *Turkish Computational and Theoretical Chemistry*, 7(3) (2023) 42-56.
- [19] B. Tüzün, Evaluation of cytotoxicity, chemical composition, antioxidant potential, apoptosis relationship, molecular docking, and MM-GBSA analysis of Rumex crispus leaf extracts. *Journal of Molecular Structure*, 1323 (2025) 140791.
- [20] H. Saraç, & B. Tüzün, Antioxidant Activity Properties of Extract of Turmeric (*Curcuma longa* L.) Plant. *Turkish Computational and Theoretical Chemistry*, 8(2) (2023) 19-27.
- [21] N. Ullah, A. Alam, B. Tüzün, N.U. Rehman, M. Ayaz, A.A. Elhenawy, ... & M. Ahmad, Synthesis of novel thiazole derivatives containing 3-methylthiophene carbaldehyde as potent anti α -glucosidase agents: In vitro evaluation, molecular docking, dynamics, MM-GBSA, and DFT studies. *Journal of Molecular Structure*, 1321 (2025) 140070.
- [22] A.D. Becke, Density-functional thermochemistry. I. The effect of the exchange-only gradient correction. *The Journal of chemical physics*, 96(3) (1992) 2155-2160.
- [23] D. Vautherin, & D.T. Brink, Hartree-Fock calculations with Skyrme's interaction. I. Spherical nuclei. *Physical Review C*, 5(3) (1972) 626.
- [24] E.G. Hohenstein, S.T. Chill, & C.D. Sherrill, Assessment of the performance of the M05-2X and M06-2X exchange-correlation functionals for noncovalent interactions in biomolecules. *Journal of Chemical Theory and Computation*, 4(12) (2008) 1996-2000.
- [25] H. Li, K. Sze, & K. Fung, Validation of inter-helical orientation of the steril-alpha-motif of human deleted in liver cancer 2 by residual dipolar couplings, protein data bank ID: 2JW2.
- [26] K. Okamoto, M. Ikemori-Kawada, A. Jestel, K. von König, Y. Funahashi, T. Matsushima, ... & J. Matsui, Distinct binding mode of multikinase inhibitor lenvatinib revealed by biochemical characterization. *ACS medicinal chemistry letters*, 6(1) (2015) 89-94.
- [27] M. McTigue, J. Wickersham, C. Pinko, Y. Hong, T. Marrone, Crystal structure of the VEGFR2 kinase domain in complex with PF-00337210 (N,2-dimethyl-6-(7-(2-morpholinoethoxy)quinolin-4-yloxy)benzofuran-3-carboxamide) (2010) PDB DOI: <https://doi.org/10.2210/pdb2xir/pdb>
- [28] R. Kong, F. Yi, P. Wen, J. Liu, X. Chen, J. Ren, ... & J.Y. Wu, Myo9b is a key player in SLIT/ROBO-mediated lung tumor suppression. *The Journal of clinical investigation*, 125(12) (2015) 4407-4420.
- [29] L.R. McLean, Y. Zhang, N. Zaidi, X. Bi, R. Wang, R. Dharanipragada, ... & D. Kominos, X-ray crystallographic structure-based design of selective thienopyrazole inhibitors for interleukin-2-inducible tyrosine kinase. *Bioorganic & medicinal chemistry letters*, 22(9) (2012) 3296-3300.
- [30] C.H. Zhou, & Y. Wang, Recent researches in triazole compounds as medicinal drugs. *Current medicinal chemistry*, 19(2) (2012) 239-280.
- [31] R. Kharb, P.C. Sharma, & M.S. Yar, Pharmacological significance of triazole scaffold. *Journal of enzyme inhibition and medicinal chemistry*, 26(1) (2011) 1-21.
- [32] C. Girmenia, & E. Finolezzi, New-generation triazole antifungal drugs: review of the phase II and III trials. 1 (2011) 1577.
- [33] J. Huo, H. Hu, M. Zhang, X. Hu, M. Chen, D. Chen, ... & Z. Wen, A mini review of the synthesis of poly-1, 2, 3-triazole-based functional materials. *RSC advances*, 7(4) (2017) 2281-2287.
- [34] R. Dennington, T.A. Keith, & J. M. Millam, (2016). *GaussView 6.0*. 16. Semichem Inc.: Shawnee Mission, KS, USA.

Volodymyr Parchenko, Alireza Poustforoosh, Yuri Karpenko, Boris Kyrychko, Burak Tüzün, Elena Kyrychko, Tatiana Chetvertak, İlayda Bersu Kul

- [35] M.J. Frisch, G.W. Trucks, H.B. Schlegel, G.R. Scuseria, M.A. Robb, J.R. Cheeseman, G. Scalmani, V. Barone, B. Mennucci, G.A. Petersson, H. Nakatsuji, M. Caricato, X. Li, H.P. Hratchian, A.F. Izmaylov, J. Bloino, G. Zheng, J.L. Sonnenberg, M. Hada, M. Ehara, K. Toyota, R. Fukuda, J. Hasegawa, M. Ishida, T. Nakajima, Y. Honda, O. Kitao, H. Nakai, T. Vreven, J.A. Montgomery, J.E. Peralta, F. Ogliaro, M. Bearpark, J.J. Heyd, E. Brothers, K.N. Kudin, V.N. Staroverov, R. Kobayashi, J. Normand, K. Raghavachari, A. Rendell, J.C. Burant S.S. Iyengar, J. Tomasi, M. Cossi, N. Rega, J.M. Millam, M. Klene, J.E. Knox, J.B. Cross, V. Bakken, C. Adamo, J. Jaramillo, R. Gomperts, R.E. Stratmann, O. Yazyev, A.J. Austin, R. Cammi, C. Pomelli, J.W. Ochterski, R.L. Martin, K. Morokuma, V.G. Zakrzewski, G.A. Voth, P. Salvador, J.J. Dannenberg, S. Dapprich, A.D. Daniels, O. Farkas, J.B. Foresman, J.V. Ortiz, J. Cioslowski, D.J. Fox, (2009) Gaussian 09, revision D.01. Gaussian Inc, Wallingford
- [36] B. Tüzün, Theoretical evaluation of six indazole derivatives as corrosion inhibitors based on DFT. Turkish computational and theoretical chemistry, 2(1) (2018) 12-22.
- [37] H. Yalazan, D. Koç, F. Aydın Kose, S. Fandaklı, B. Tüzün, M.İ. Akgül, ... & H. Kantekin, Design, syntheses, theoretical calculations, MM-GBSA, potential anti-cancer and enzyme activities of novel Schiff base compounds. Journal of Biomolecular Structure and Dynamics, 42(23) (2024) 13100-13113.
- [38] Schrödinger Release 2022-4: Maestro, Schrödinger, LLC, New York, NY, 2022.
- [39] I. Shahzadi, A.F. Zahoor, B. Tüzün, A. Mansha, M.N. Anjum, A. Rasul, ... & M. Mojzych, Repositioning of acefylline as anti-cancer drug: Synthesis, anticancer and computational studies of azomethines derived from acefylline tethered 4-amino-3-mercapto-1, 2, 4-triazole. Plos one, 17(12) (2022) e0278027.
- [40] M. El Faydy, L. Lakhri, N. Dahiieh, K. Ounine, B. Tüzün, N. Chahboun, ... & A. Zarrouk, Synthesis, Biological Properties, and Molecular Docking Study of Novel 1, 2, 3-Triazole-8-quinolinol Hybrids. ACS omega, 9(23) (2024) 25395–25409.
- [41] Schrödinger Release 2022-4: Protein Preparation Wizard; Epik, Schrödinger, LLC, New York, NY, 2022; Impact, Schrödinger, LLC, New York, NY; Prime, Schrödinger, LLC, New York, NY, 2022
- [42] Schrödinger Release 2022-4: LigPrep, Schrödinger, LLC, New York, NY, 2022.
- [43] Schrödinger Release 2022-4: QikProp, Schrödinger, LLC, New York, NY, 2022.
- [44] Poustforoosh, A., Faramarz, S., Nematollahi, M. H., Mahmoodi, M., & Azadpour, M. (2024). Correction: Structure-Based Drug Design for Targeting IRE1: An in Silico Approach for Treatment of Cancer. Drug Research, 74(02), e1-e1.
- [45] A. Poustforoosh, The impact of cationic/anionic ratio on the physicochemical aspects of catanionic niosomes as a promising carrier for anticancer drugs. Journal of Molecular Liquids, (2024) 125338.
- [46] A. Poustforoosh, Investigation on the structural and dynamical properties of cationic, anionic, and catanionic niosomes as multifunctional controlled drug delivery system for cabozantinib. Colloids and Surfaces A: Physicochemical and Engineering Aspects, 687 (2024) 133547.
- [47] A. Boris, V.V. Parchenko, E.G. Knysh, & A.G. Kaplaushenko, Development of hplc-esi-ms method for determining morpholinium 2-(5-(pyridine-4-yl)-1, 2, 4-triazole-3-yltio) acetate in bird eggs.
- [48] N.D. Greer, Voriconazole: the newest triazole antifungal agent. Proc (Bayl Univ Med Cent) 16(2) (2003) 241-8.
- [49] H. Yalazan, D. Koç, F. Aydın Kose, M.İ. Akgül, S. Fandaklı, B. Tüzün, ... & H. Kantekin, Chalcone-based schiff bases: Design, synthesis, structural characterization and biological effects. Journal of Molecular Structure, 1337 (2025) 142211.
- [50] S. Manap, H. Medetalibeyoğlu, A. Kılıç, O.F. Karataş, B. Tüzün, M. Alkan, ... & H. Yüksek, Synthesis, molecular modeling investigation, molecular dynamic and ADME prediction of some novel Mannich bases derived from 1, 2, 4-triazole, and assessment of their anticancer activity.

Volodymyr Parchenko, Alireza Poustforoosh, Yuri Karpenko, Boris Kyrychko, Burak Tüzün, Elena Kyrychko, Tatiana Chetvertak, İlayda Bersu Kul

- Journal of Biomolecular Structure and Dynamics, 42(21) (2024) 11916-11930.
- [51] O. Myroslava, A. Poustforoosh, B. Inna, V. Parchenko, B. Tüzün, & B. Gutyj, Molecular descriptors and in silico studies of 4-((5-(decylthio)-4-methyl-4n-1, 2, 4-triazol-3-yl) methyl) morpholine as a potential drug for the treatment of fungal pathologies. *Computational Biology and Chemistry*, 113 (2024) 108206.
- [52] A. Rafik, B. Tuzun, H. Zouihri, A. Poustforoosh, R. Hsissou, A. Elhenaey, & T. Guedira, Morphology studies, optic proprieties, hirschfeld electrostatic potential mapping, docking molecular anti-inflammatory, and dynamic molecular approaches of hybrid phosphate. *Journal of the Indian Chemical Society*, 101(11) (2024) 101419.
- [53] N. Barghady, S.A. Assou, M. Er-Rajy, K. Boujdi, A. Arzine, Y. Rhazi, ... & M. El Yazidi, Design, synthesis, characterization, and theoretical calculations, along with in silico and in vitro antimicrobial proprieties of new isoxazole-amide conjugates. *Open Chemistry*, 22(1) (2024) 20240109.
- [54] A.K. Goswami, M.A. Aboul-Soud, N. Gogoi, M. El-Shazly, J.P. Giesy, B. Tüzün, ... & H.K. Sharma, Integrative in silico evaluation of the antiviral potential of terpenoids and its metal complexes derived from Homalomena aromatica based on main protease of SARS-CoV-2. *Open Chemistry*, 22(1) (2024) 20240085.
- [55] Ü.M., Koçyiğit, M. Doğan, H. Muğlu, P. Taslimi, B. Tüzün, H. Yakan, ... & İ. Gülçin, Determination of biological studies and molecular docking calculations of isatin-thiosemicarbazone hybrid compounds. *Journal of Molecular Structure*, 1264 (2022) 133249.
- [56] F. Türkan, P. Taslimi, B. Cabir, M.S. Ağırtas, Y. Erden, H.U. Celebioglu, ... & I. Gulcin, Co and Zn Metal phthalocyanines with bulky substituents: anticancer, antibacterial activities and their inhibitory effects on some metabolic enzymes with molecular docking studies. *Polycyclic Aromatic Compounds*, 42(7) (2022) 4475-4486.
- [57] M.R. Taysi, M. Kirici, M. Kirici, B. Tuzun, & A. Poustforoosh, Antioxidant enzyme activities, molecular docking studies, MM-GBSA, and molecular dynamic of chlorpyrifos in freshwater fish *Capoeta umbla*. *Journal of biomolecular structure and dynamics*, 42(1) (2024) 163-176.
- [58] A.H.T. Kafa, G. Tüzün, E. Güney, R. Aslan, K. Sayın, B. Tüzün, & H. Ataseven, Synthesis, computational analyses, antibacterial and antibiofilm properties of nicotinamide derivatives. *Structural Chemistry*, 33(4) (2022) 1189-1197.
- [59] H. Medetalibeyoğlu, S. Manap, M. Alkan, M. Beytur, N. Barlak, O.F. Karatas, ... & P. Taslimi, Novel Schiff Bases: Synthesis, Characterization, Bioactivity, Cytotoxicity, and Computational Evaluations. *Polycyclic Aromatic Compounds*, (2024) 1-19.
- [60] M. Tapera, H. Kekeçmuhammed, B. Tüzün, S.D. Daştan, M.S. Çelik, P. Taslimi, ... & E. Sarıpınar, Novel 1, 2, 4-triazole-maleamic acid derivatives: synthesis and evaluation as anticancer agents with carbonic anhydrase inhibitory activity. *Journal of Molecular Structure*, 1313 (2024) 138680.
- [61] A. Mermer, M.V. Bulbul, S.M. Kalender, I. Keskin, B. Tuzun, & O.E. Eyupoglu, Benzotriazole-oxadiazole hybrid Compounds: Synthesis, anticancer Activity, molecular docking and ADME profiling studies. *Journal of Molecular Liquids*, 359 (2022) 119264.
- [62] A. Poustforoosh, & F. Moosavi, Evaluation of the FDA-approved kinase inhibitors to uncover the potential repurposing candidates targeting ABC transporters in multidrug-resistant cancer cells: an in silico approach. *Journal of Biomolecular Structure and Dynamics*, 42(24) (2024) 13650-13662.